Molecular Recognition

DOI: 10.1002/anie.200902490

What is Cooperativity?

Christopher A. Hunter and Harry L. Anderson**

allosteric cooperativity · chelate cooperativity · cooperative effects · self-assembly · supramolecular chemistry

Dedicated to Professor Jean-Marie Lehn on the occasion of his 70th birthday

1. Introduction: It's All or Nothing

Cooperativity is a central concept for understanding molecular recognition and supramolecular self-assembly,[1–3] yet there is widespread confusion about the definition and quantification of cooperativity, particularly in the context of self-assembled structures.[4–7] Herein, we delineate two types of cooperativity—allosteric and chelate cooperativity—in multivalent systems. Allosteric cooperativity is widely recognized, whereas the significance of chelate cooperativity has been overlooked.

Cooperativity arises from the interplay of two or more interactions, so that the system as a whole behaves differently from expectations based on the properties of the individual interactions acting in isolation. Coupling of interactions can lead to positive or negative cooperativity, depending on whether one interaction favors or disfavors another. Cooperativity is the key feature of systems chemistry that leads to collective properties not present in the individual molecular components. It is one of the most important properties of the molecular systems found in biology.[8]

Text books often quote two archetypal examples of cooperativity: the binding of oxygen to hemoglobin,[1] in which binding at each of the four sites increases the oxygen affinity of the other sites (Figure 1a), and the folding of biopolymers (e.g., protein, DNA, or RNA), characterized by sharp melting transitions (Figure 1b).[9] Supramolecular self-assembly processes display similar behavior (Figure 1c). The relationship between these different types of cooperativity has not been well defined, and is the subject of this Essay.

The three equilibria portrayed in Figure 1a–c shift in response to changes in conditions (Figure 1d, horizontal axis):

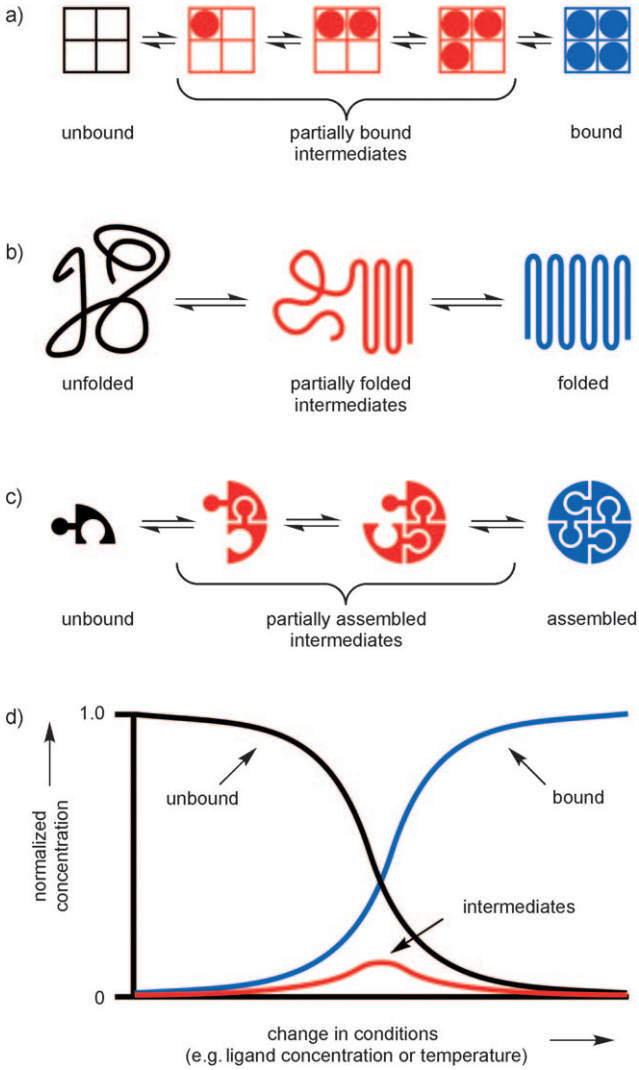

Figure 1. Representation of processes that display positive cooperativity: a) hemoglobin binding oxygen, b) protein folding, and c) supramolecular self-assembly. d) Speciation profiles. Positive cooperativity leads to a low peak concentration of intermediates and a sharp transition from unbound to bound.

oxygen concentration for hemoglobin, denaturant concentration or temperature for biopolymer folding, and concentration or temperature for supramolecular assembly. Positive cooperativity implies a low concentration of intermediates

[*] Prof. C. A. Hunter
Department of Chemistry, University of Sheffield
Sheffield S3 7HF (UK)
Fax: (+44) 114-222-9346
E-mail: c.hunter@shef.ac.uk
Homepage: http://www.chris-hunter.staff.shef.ac.uk/
Prof. H. L. Anderson
Department of Chemistry, University of Oxford
Oxford OX1 3TA (UK)
Fax: (+44) 1865-285-002
E-mail: harry.anderson@chem.ox.ac.uk
Homepage: http://hla.chem.ox.ac.uk/

Supporting information for this article is available on the WWW under http://dx.doi.org/10.1002/anie.200902490.

(partially bound, folded, or assembled; red in Figure 1). In other words, as the system approaches the limit of strong positive cooperativity, only the extreme states are significantly populated. Such systems can exhibit "all-or-nothing" behavior in two senses:

1) *At the molecular level*: any individual molecule is likely to be fully bound or fully unbound; it spends little time in intermediate states.
2) *At the macroscopic level*: the behavior of the ensemble is characterized by a population switch from mainly free to mainly bound over a small change in conditions. Under most conditions, one state predominates, and this leads to the sigmoidal binding isotherms and sharp melting transitions that are the classical signatures of cooperativity, as illustrated by the binding of oxygen to hemoglobin[1,10] and the denaturation of lysozyme in Figure 2.[11]

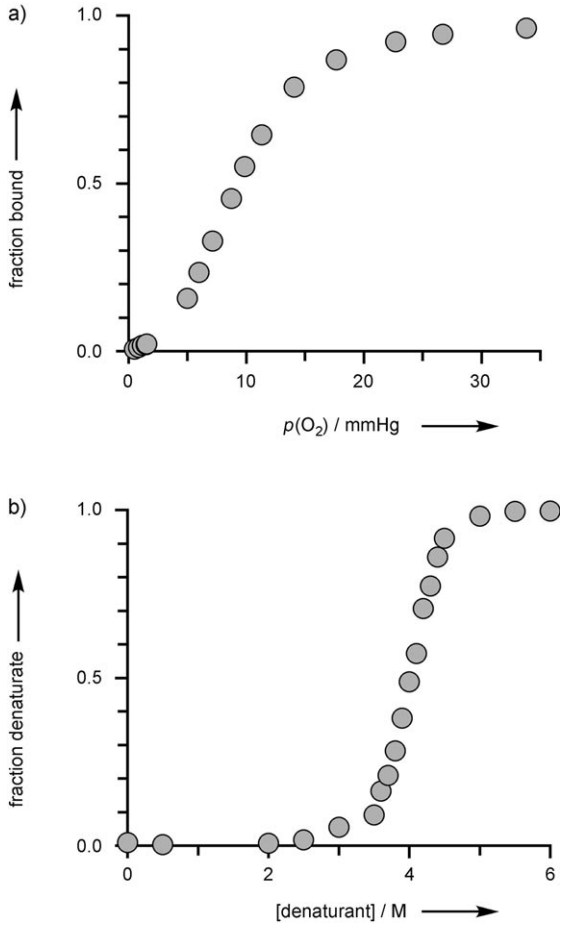

Figure 2. Experimentally observed isotherms for a) oxygen binding by hemoglobin as a function of oxygen concentration[10] and b) the denaturation of lysozyme as a function of guanidine hydrochloride concentration.[11]

All-or-nothing behavior is the key consequence of positive cooperativity. It occurs widely in biology: switching between "on" and "off" states results from a small change in conditions. Intermediate structures, which may have undesirable properties, are not populated.

2. Thermodynamic Models

In general, we may consider the multicomponent complexes formed between multidentate ligands and multisite receptors. A wide variety of different supramolecular architectures is possible, and coupling between the multiple intermolecular interactions present in these complexes generates different kinds of cooperative behavior. Here we explore the principles by discussing the scenarios (a)–(e) summarized in Figure 3. In each case, we start by considering simple equilibria that involve molecules with only one or two binding sites, then extrapolate to cases with many interactions. A detailed mathematical analysis of the thermodynamic models discussed here is included in the Supporting Information.

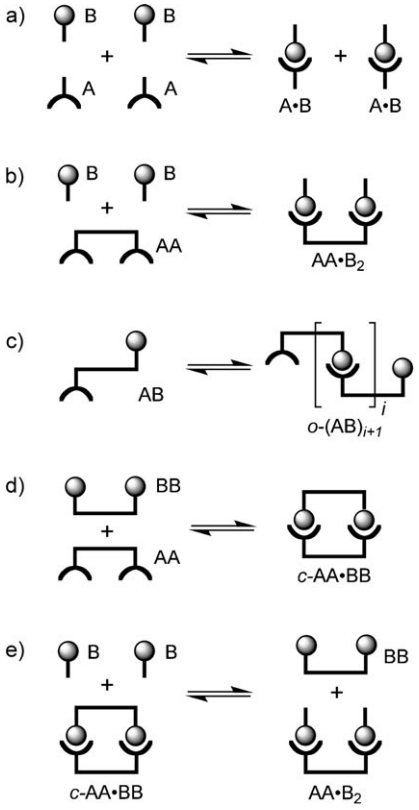

Figure 3. Complexation equilibria involving molecules with one or two binding sites. a) The reference system. b) Discrete allosteric systems. c) Polydisperse oligomerization. d) Self-assembled systems. e) Denaturation.

2.1. The Reference System

We start by considering a system where there can be no cooperativity because there is only one interaction. The complex between a receptor with one binding site (A) and a ligand with one binding site (B; Figure 3a) is our reference point for assessing other scenarios. This simple two-state equilibrium is characterized by the association constant K [Eq. (1)], where [A·B] and [A] are the concentrations of

bound and free receptor, and [B] is the concentration of free ligand.

$$K = \frac{[A \cdot B]}{[A]\ [B]} \quad (1)$$

2.2. Allosteric Ligand Binding

This scenario is the type of cooperativity exhibited by hemoglobin. The simplest case of two ligands, each with one binding site, that interact with a receptor with two covalently connected binding sites is illustrated in Figure 4a. The receptor has three possible states: free AA, partially bound AA·B, and fully bound AA·B_2. The equilibria are characterized by two microscopic association constants K_1 and K_2, which are defined by Equations (2) and (3). The statistical factor of two reflects the degeneracy of the partially bound intermediate.[12]

$$2\,K_1 = \frac{[AA \cdot B]}{[AA]\ [B]} \quad (2)$$

$$\tfrac{1}{2}K_2 = \frac{[AA \cdot B_2]}{[AA \cdot B]\ [B]} \quad (3)$$

At the molecular level, the cooperativity of the system is described by the interaction parameter α, which is defined by Equation (4).[13] In the absence of cooperativity, the microscopic association constants are identical to the value for the corresponding reference receptor with one binding site, that is, $K_1 = K_2 = K$ and $\alpha = 1$.

$$\alpha = \frac{K_2}{K_1} \quad (4)$$

Under a given set of conditions, the total fraction of receptor sites that are bound to ligand is defined as the binding-site occupancy of the receptor θ_A, which is given by Equation (5), where $[AA]_0$ is the total receptor concentration (free and bound). It is often easier to measure θ_A than to determine the concentrations of all the different species present in equilibrium, and, from a theoretical perspective, the description of complex equilibria in terms of θ_A leads to a dramatic simplification.

$$\theta_A = \frac{\tfrac{1}{2}[AA \cdot B] + [AA \cdot B_2]}{[AA]_0} \quad (5)$$

Speciation curves, which show how [AA·B], [AA·B_2], and θ_A vary with $[B]_0$, are plotted for three different cooperativity regimes in Figure 4b–d, with $\alpha = 1$, 0.01, and 100 (in these plots, $K'[B]_0$ is a normalized concentration scale).[14] In each case, the site-occupancy (θ_A) profile of the two-site receptor (black curve) is compared with that of the one-site reference receptor (gray dots).

No cooperativity ($\alpha = 1$, Figure 4b). In this regime $K_1 = K_2$, and the θ_A curve is identical to that of the one-site reference system.

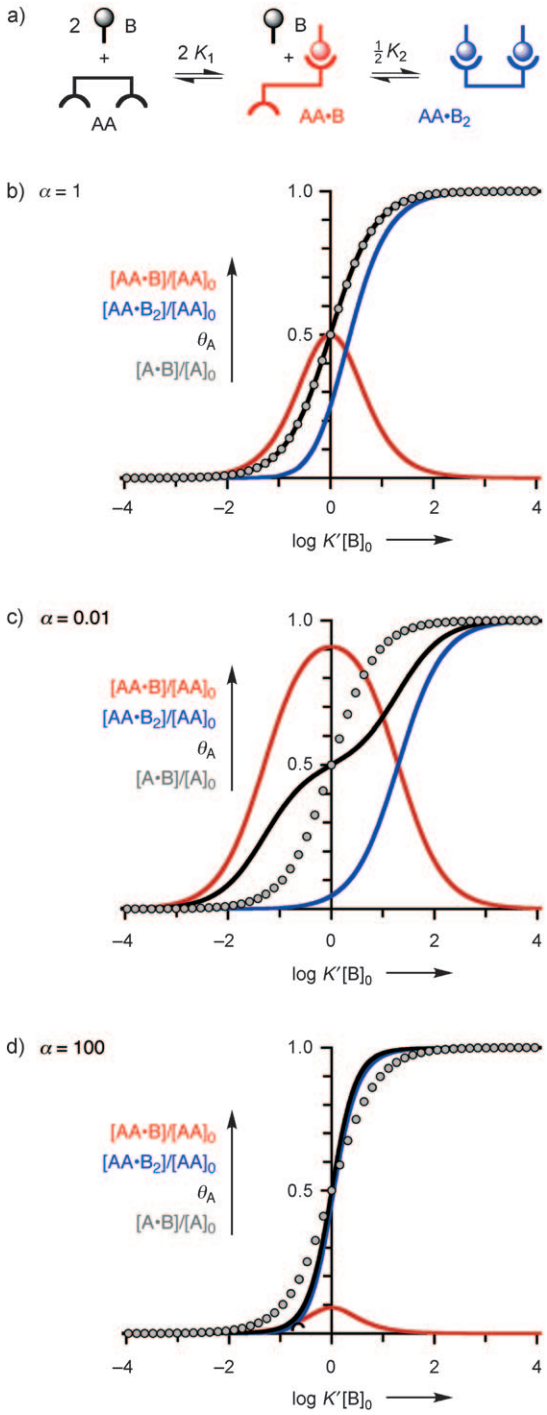

Figure 4. a) Interaction of a monovalent ligand B with a two-site receptor AA.[12] Speciation profiles for b) $\alpha = 1$; c) $\alpha = 0.01$; and d) $\alpha = 100$ (fully bound AA·B_2 in blue; intermediate AA·B in red, and total binding site occupancy θ_A in black; $[B]_0 = [B] + [AA \cdot B] + 2[AA \cdot B_2]$). The speciation profile for the reference system with one binding site is also shown (gray dots). In (d), the population of AA·B_2 and θ_A are practically identical. In all cases, curves are calculated assuming, for mathematical simplicity, that $[B]_0 \gg [AA]_0$.[14]

Negative cooperativity ($\alpha < 1$, Figure 4c). Here $K_1 > K_2$, and the intermolecular interaction in the intermediate AA·B is stronger than in the fully bound state AA·B_2. Formation of the fully bound complex takes place over a wider concen-

tration range than for the one-site reference receptor. The intermediate AA·B is the dominant species at intermediate concentrations, and in the limit of $\alpha \ll 1$, the fully bound state is never populated.

Positive cooperativity ($\alpha > 1$, Figure 4d). In this case, $K_1 < K_2$, and the interactions in the fully bound state are more favorable than in the intermediate. In the limit of $\alpha \gg 1$, the intermediate is never populated, and all-or-nothing, two-state behavior is observed. Assembly and disassembly of the complex take place over a narrower range of concentrations than for the single-site reference system.

At the macroscopic level, cooperativity in allosteric systems is usually characterized by plotting $\log\{\theta_A/(1-\theta_A)\}$ versus $\log[B]_0$ in a Hill plot.[15] The *Hill coefficient* n_H is the slope of this plot measured at 50% saturation, that is, at $\log\{\theta_A/(1-\theta_A)\}=0$. A simple reference receptor with one binding site gives $n_H=1$; any deviation from this value indicates cooperative behavior, as illustrated in Figure 5a by constructing Hill plots for the three regimes of Figure 4b–d. Negative cooperativity (red line) gives a slope of less than 1 at the origin ($n_H<1$), while positive cooperativity (blue line) leads to a slope of more than 1 at the origin ($n_H>1$). At the extremes of the Hill plot, the slope returns to 1, because changes in θ_A are caused by only the first binding event at low ligand concentrations, and only the second binding event at high ligand concentrations.

The macroscopic behavior of systems of this type can also be characterized by the *switching window* c_R [Eq. (6)], which

$$c_R = \frac{[B]_0 \text{ at } \theta_A = 10/11}{[B]_0 \text{ at } \theta_A = 1/11} \tag{6}$$

is the factorial increase in ligand concentration required to change the bound/free receptor ratio from 1:10 to 10:1 (Figure 5b).[16] In other words, c_R is a measure of the sharpness of the bound–free transition. For the simple one-site reference receptor, $\log c_R = 2$, and any deviation from this value indicates cooperative behavior, as illustrated in Figure 5b for the examples from Figure 4. Positive cooperativity (blue line) reduces the value of c_R, that is, the bound–free switch takes place over a narrow concentration range. The opposite is true for negative cooperativity (red line), which leads to separation of the two binding events on the concentration scale.

The relationship between the molecular parameter α and the macroscopic parameters n_H and c_R is illustrated in Figure 6. At the non-cooperative reference point, $\alpha=1$, $n_H=1$, and $\log c_R = 2$. For systems that exhibit modest cooperativity, the value of n_H depends strongly on α. At the extremes, n_H tends to a value of zero for strong negative cooperativity ($\alpha \ll 1$) and to a value of two for strong positive cooperativity ($\alpha \gg 1$). In contrast, $\log c_R$ decreases as α increases, and tends to a limit of one for systems with strong positive cooperativity. In the negative cooperativity regime, the value of c_R is inversely proportional to α, as the first and second binding events simply move further apart on the concentration axis.

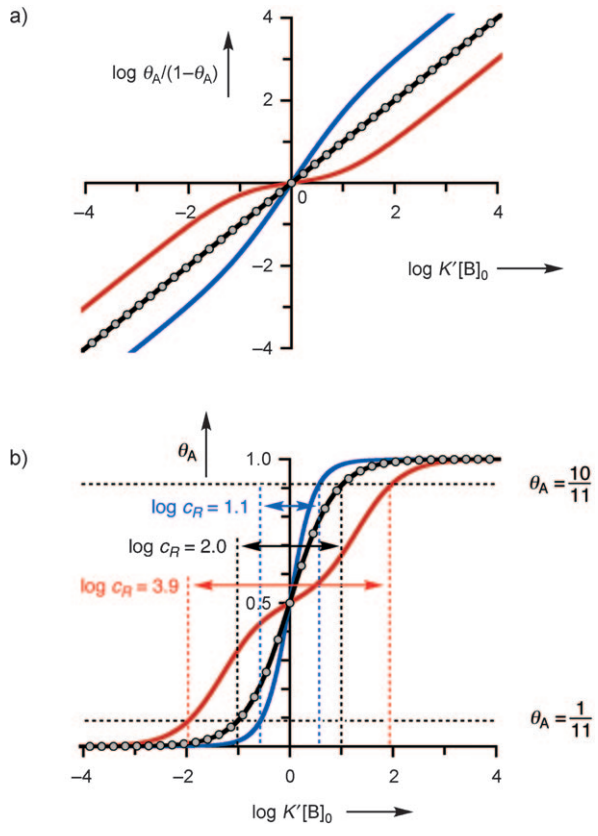

Figure 5. Plots for determining a) the Hill coefficient n_H and b) the switching window c_R for two monovalent ligands (B) that interact with a two-site receptor (AA). Three regimes are illustrated: no cooperativity ($\alpha=1$ in black), negative cooperativity ($\alpha=0.01$ in red), and positive cooperativity ($\alpha=100$ in blue). Data for the single-site receptor are shown for reference (gray dots).[14]

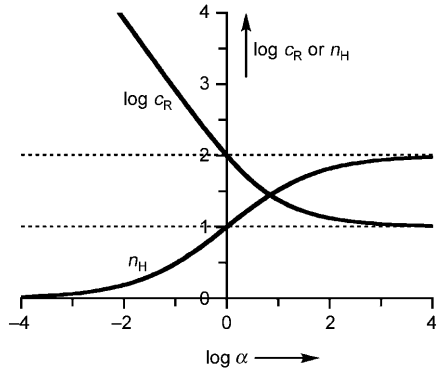

Figure 6. Relationship between the molecular parameter α and macroscopic parameters n_H and c_R for binding a monovalent ligand to a two-site receptor.

The properties of this two-site system can be generalized to receptors with a large number (N) of binding sites (Figure 7). The number of possible intermediates increases with N, as do the number of independent association constants. We will consider the three limiting regimes:

No cooperativity ($\alpha=1$). In this regime, the macroscopic behavior of the system is effectively independent of N.

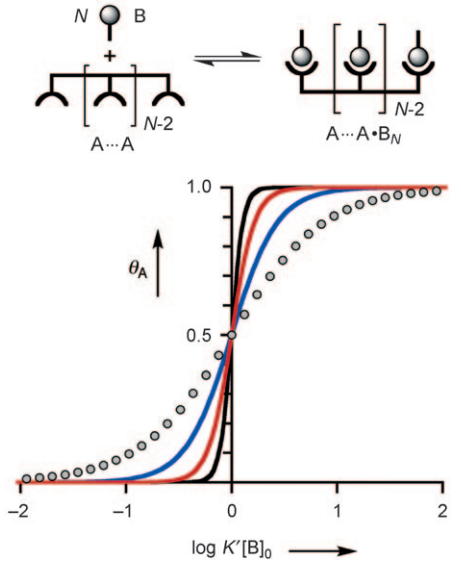

Figure 7. Binding of N monovalent ligands (B) to a receptor with N binding sites (A···A). There are many possible partially bound intermediate states, but they will not be significantly populated if the system displays strong positive allosteric cooperativity. Binding isotherms are shown for this equilibrium in the regime of strong positive allosteric cooperativity ($\alpha \gg 1$). $N=1$ gray dots, $N=2$ blue, $N=4$ red, $N=8$ black.[14]

Although the speciation profiles are complicated by a large number of intermediates, the concentration dependence of the site occupancy (θ_A) is identical to the one-site reference system; $n_H=1$ and $\log c_R=2$.

Negative cooperativity ($\alpha<1$). Similarly, the only change that occurs on increasing N is an increase in the number of intermediate states. The concentration range over which these states are populated is extended.

Positive cooperativity ($\alpha>1$). In this regime, the properties of the system are strongly dependent on N. Figure 7 illustrates the influence of N on the binding isotherm in the limit of strong positive cooperativity with $N=2$, 4, and 8. The transition between free and bound states takes place over a progressively narrower concentration window as N increases. In the limit of high α, $\log c_R$ tends to $2/N$, and n_H tends to N.[17] As a consequence, the large number of potential intermediates that proliferate as N is increased are never populated, and two-state all-or-nothing behavior is observed at the molecular level. In the limit of large N and large α values, the switch between the free and bound states of the receptor can be achieved with a small change in the concentration of ligand, so the systems displays macroscopic all-or-nothing behavior.

Allosteric cooperativity has been extensively studied in biological systems, such as oxygen binding to hemoglobin,[1] and peptide binding to the vancomycin dimer.[18] Many mechanisms can result in positive or negative allosteric cooperativity, for example, conformational changes,[2,19] electronic polarization of the receptor,[20] or long-range electrostatic interactions between the ligands.[18] The most trivial cause for negative cooperativity is steric repulsion between two bound ligands. The details are beyond the scope of this Essay, but in general, *positive cooperativity can be achieved either by making the first binding event less favorable or by making subsequent binding events more favorable.*

2.3. Nucleation–Growth of Polydisperse Open Oligomers

Cooperative oligomerization is important in the aggregation of amyloid peptides,[21] actin strands,[22] and supramolecular polymers.[23] These processes can be understood by considering the simple model shown in Figure 3c and 8a, in which monomer AB self-associates to give a distribution of oligomers $(AB)_i$, where $i=1-\infty$. If all of the stepwise association constants are identical ($K_i=K$), a concentration-dependent statistical mixture of oligomers, known as an isodesmic distribution, is formed. The θ_A binding isotherm for this type of non-cooperative process is identical to that for dilution of a 1:1 mixture of A and B, the reference system (Figure 8, black line and gray points).

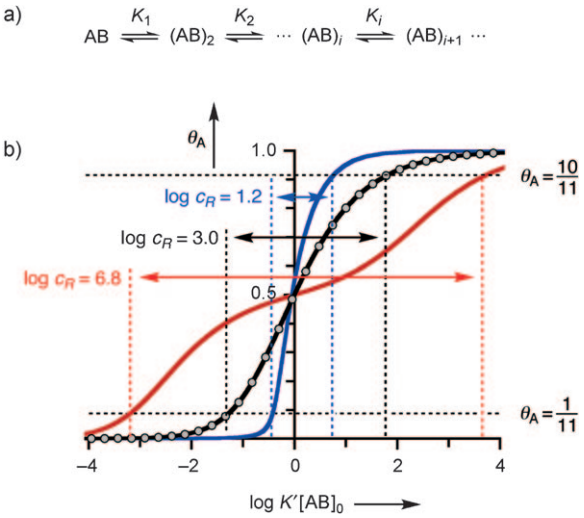

Figure 8. a) General representation for oligomerization of a self-complementary molecule AB. b) Binding isotherms for $\alpha=1$ black, $\alpha=0.01$ red, $\alpha=100$ blue, showing measurements of the corresponding concentration switching windows c_R ($K_i=K_2$ for all $i>1$ and $\alpha=K_2/K_1$). The binding isotherm for dilution of a 1:1 mixture of A and B is shown for reference (gray dots).[14]

In principle, any distribution of association constants is possible. We will consider a simple scenario that leads to the observation of macroscopic cooperativity in the formation of polydisperse open-chain aggregates:[22,24] all of the association constants for adding monomer units to oligomeric chains are identical (K_2), except for the formation constant for the dimer $(AB)_2$, which is K_1. As before, the allosteric interaction parameter is defined as $\alpha=K_2/K_1$. Three regimes can be identified (Figure 8b):

No cooperativity ($\alpha=1$). Isodesmic growth with a statistical distribution of oligomers.

Negative cooperativity ($\alpha<1$). The dimer is the most stable species, so that oligomerization does not take place until high concentrations of AB are reached.

Positive cooperativity ($\alpha > 1$). The dimer is the least stable species and is not significantly populated. Dimer formation constitutes a nucleation step; subsequent oligomerization takes place over a narrow concentration window and the system shows macroscopic cooperativity. Thus the major species that are populated are monomer and long oligomers.

Although the binding isotherms in Figure 8b appear similar to those for the allosteric receptor–ligand systems (Figure 5b), the oligomerization isotherm is not symmetric about the origin on the concentration scale. The reason is that self-association is studied by dilution experiments rather than titrations: when the ligand is present in excess, as in a titration experiment, it is almost all free ($[B] \approx [B]_0$), but at high concentrations of AB in a dilution experiment most of the AB is bound ($[AB] \ll [AB]_0$). Hill plots are problematic for dilution experiments: the slope for the non-cooperative isodesmic system is not constant and does not have a maximum at 50% saturation (see the Supporting Information). However, the concentration switching window c_R can be used as a macroscopic measure of cooperativity in dilution experiments. The only difference from titration experiments is that $\log c_R = 3$ for the non-cooperative isodesmic system. Any deviation from this value indicates cooperative behavior. In the limit of strong positive cooperativity ($\alpha \gg 1$), $\log c_R$ tends a value of 1: a sharp nucleation point is observed followed by growth of oligomers, and a 10-fold increase in concentration is required to reach 90% saturation.

There are many different molecular mechanisms that give rise to this type of cooperative oligomerization. For example, in helical aggregates, the *i*th monomer unit can have a favorable contact interaction with the $(i-2)$th monomer unit.[22] In H-bonded urea aggregates, the *i*th monomer unit has a favorable noncontact interaction, which is mediated by polarization, with the $(i-2)$th monomer unit.[25] The nucleation and growth behavior in Figure 8 has been studied by Meijer and co-workers in the context of very large H-bonded assemblies.[23] As with discrete allosteric systems, *positive allosteric cooperativity is achieved by making initial binding events less favorable or by making later binding events more favorable.*

2.4. Self-Assembly of Closed Systems

Now we turn to the type of cooperativity observed in protein folding or DNA duplex formation and consider the consequences of allowing some of the interactions to become intramolecular. The simplest case of two molecules that each have two binding sites is illustrated in Figure 9. This system is more complicated than the allosteric systems in Figure 4, because there are more possible bound states. However, if the ligand is present in a large excess relative to the receptor, then we can ignore complexes that involve more than one receptor, because they will not be significantly populated. Under these conditions, there are only four states for the receptor (highlighted in the box in Figure 9): free AA, two 1:1 complexes (the partially bound open intermediate *o*-AA·BB and the fully bound cyclic complex *c*-AA·BB), and the 2:1 complex

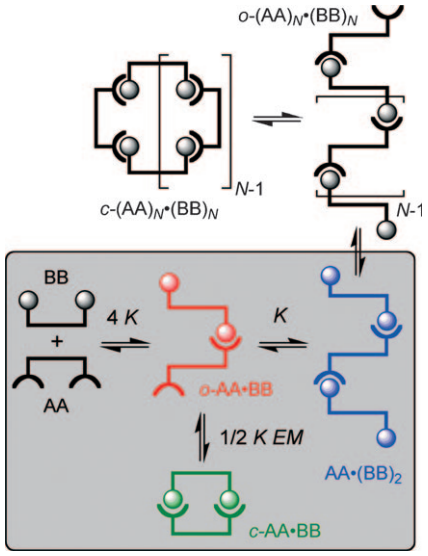

Figure 9. A two-site receptor (AA) that interacts with a divalent ligand (BB), assuming $\alpha = 1$.[12] Many states are possible for this system, but if $[BB]_0 \gg [AA]_0$, only the species inside the box are populated.

AA·$(BB)_2$. Here we limit ourselves to the scenario where $\alpha = 1$ and there is no allosteric cooperativity.

At the molecular level, the key feature that defines the properties of this system is the intramolecular binding interaction that leads to the cyclic 1:1 complex *c*-AA·BB. This interaction is described using the effective molarity (*EM*) as defined in Equation (7).[26]

$$\frac{1}{2} K\,EM = \frac{[c\text{-AA}\cdot\text{BB}]}{[o\text{-AA}\cdot\text{BB}]} \tag{7}$$

As implied by this equation, the ratio of the open and closed 1:1 complexes is independent of the ligand concentration. The product $K\,EM$ determines the extent to which the cyclic complex is populated, and is the key molecular parameter that defines the cooperativity of self-assembled systems. Two regimes are considered in Figure 10.

KEM $\ll 1$ (Figure 10a). Under these conditions, the partially bound intermediate is more stable than the cyclic complex. The system is unaffected by the presence of the cyclic complex, and the behavior is identical to that found for monovalent ligands (compare Figure 4b and Figure 10a).

KEM $\gg 1$ (Figure 10b). In this case, the cyclic complex is more stable than the partially bound intermediate, and *c*-AA·BB is the major species over a wide concentration range. The open partially bound intermediate *o*-AA·BB is barely populated, and formation of the 2:1 complex AA·$(BB)_2$ is suppressed compared to the situation with the corresponding monovalent ligands. The cyclic 1:1 complex *c*-AA·BB opens to form the 2:1 complex AA·$(BB)_2$ only when $2[BB]_0 > EM$. In other words, *EM* defines the concentration at which simple monovalent intermolecular interactions compete with cooperative intramolecular ones. If we compare the speciation profile with that of the one-site reference system (gray dots in Figure 10b), it is clear that the intramolecular interaction significantly increases the overall

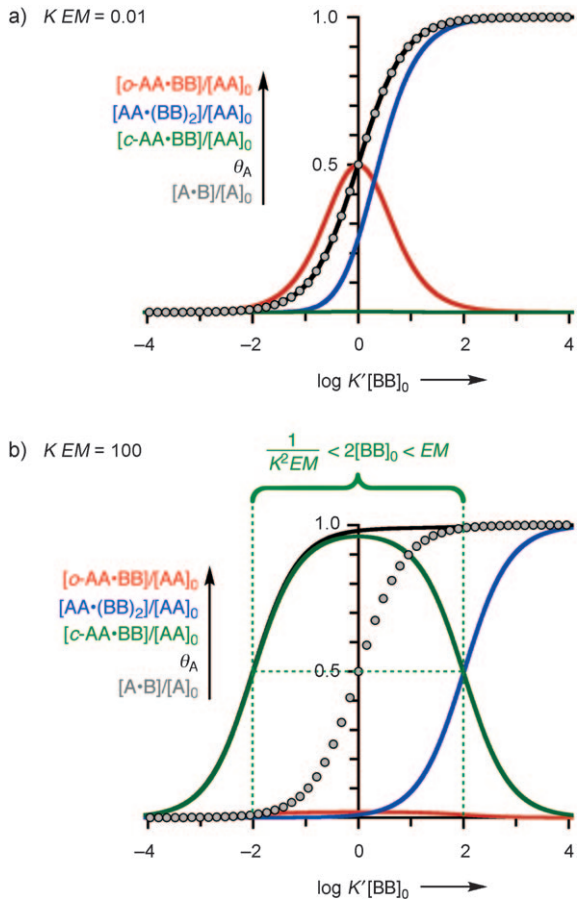

Figure 10. Speciation profiles for the equilibria shown in Figure 9 (cyclic complex *c*-AA·BB in green, open intermediate *o*-AA·BB in red, 2:1 complex AA·$(BB)_2$ in blue, and total binding-site occupancy θ_A in black). a) $KEM = 0.01$ and b) $KEM = 100$. In both cases, $\alpha = 1$. The speciation profile for the system with one intermolecular interaction is shown for reference (gray dots).[14,27]

stability of the complex at low ligand concentrations. The cyclic complex is the dominant species (>50%) over a concentration window [Eq. (8)]:

$$(K^2\,EM)^{-1} < 2[\mathrm{BB}]_0 < EM \qquad (8)$$

In these examples $\alpha = 1$, but in general, the allosteric interaction parameter may deviate from 1, and this modifies the behavior of self-assembled systems. Changes in α do not affect the ligand concentration window over which the cyclic complex *c*-AA·BB is populated, but they perturb the equilibrium between the open and cyclic 1:1 complexes.

This system displays a different kind of cooperativity from that discussed above for allosteric systems. Cooperative assembly of the complex is driven by the difference in strength between the intermolecular and intramolecular interactions, and is a consequence of the molecular architecture. This phenomenon gives rise to the chelate effect,[28] so we call it chelate cooperativity. This is the type of cooperativity exhibited in the folding of proteins and supramolecular self-assembly (Figure 1b,c).

Cooperativity in this system is expressed at the molecular level, with all-or-nothing population of the cyclic complex in the limit of strong chelate cooperativity. However, the macroscopic parameters used to characterize allosteric cooperativity n_H and c_R do not provide an insight into cooperativity in the *c*-AA·BB complex: $n_H = 1$ and $\log c_R = 2$ for all of the examples shown in Figure 10. Therefore it can be difficult to recognize the cooperativity present in self-assembled systems.

The behavior of the two-site system shown in Figure 9 can be extrapolated to a larger number (N) of interaction sites in a variety of ways. Here we consider two architectures: firstly, we keep the stoichiometry of the complex at 1:1 and increase the number of binding sites on both components (Figure 11);

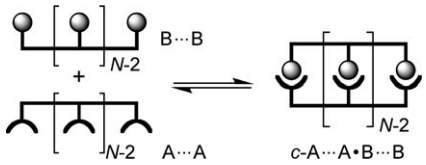

Figure 11. Self-assembly of a 1:1 complex of a polytopic receptor (A···A) and a complementary polyvalent ligand (B···B). There are many other possible states, but they will not be significantly populated if the system displays strong chelate cooperativity ($KEM \gg 1$).

secondly, we increase the number of molecules in the complex, while keeping two binding sites per molecule (Figure 12). The former architecture illustrates the kind of cooperativity observed in the assembly of a DNA duplex, while the latter corresponds to the cooperativity in the self-assembly of a multicomponent complex, such as a virus capsule.

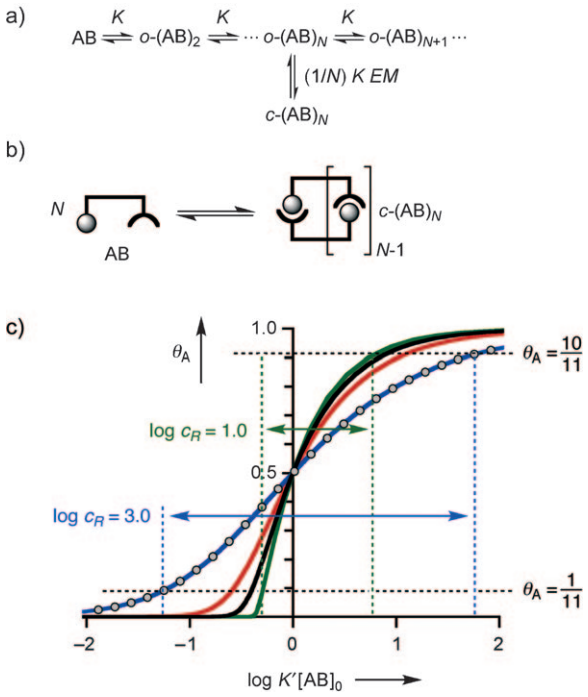

Figure 12. a) Self-assembly of AB oligomers where one open oligomer can cyclize ($\alpha = 1$).[12] b) If the system displays strong chelate cooperativity, *c*-$(AB)_N$ is the dominant bound state. c) Binding isotherms for $N = 2$ blue, $N = 4$ red, $N = 8$ black, $N = 30$ green ($KEM \gg 1$).[14]

1) **Interaction of an oligomeric ligand with an oligomeric receptor**. The number of possible partially bound intermediates increases with the number of binding sites. The population of each intermediate depends on the product KEM for the relevant intramolecular interaction. However, in the limit of $KEM \gg 1$, no intermediates are formed, and two-state all-or-nothing behavior is observed (Figure 11). The overall stability of the complex increases as N is increased, but the shape of the binding isotherm is independent of N, because this case is simply a 1:1 complexation process ($n_H = 1$ and $\log c_R = 2$). Here, the all-or-nothing behavior is molecular but not macroscopic, and the concentration dependence of the free-bound transition is no sharper than that for an isolated one-site interaction. Macroscopic cooperativity can however be observed by thermal or chemical denaturing of the *c*-A···A·B···B duplex (see below).
2) **Closed oligomeric assemblies of a self-complementary molecule.** These systems represent a special case of the oligomerization of AB illustrated in Figure 8a. Section 2.3 dealt with polydisperse open-chain aggregates of AB, but if an oligomer of a particular size has a significant tendency to cyclize, then this cyclic oligomer can become a thermodynamic sink (Figure 12a). In the limit of $KEM \gg 1$ (where EM is the effective molarity for cyclization of a specific linear oligomer o-$(AB)_N$), the system reduces to a two-state equilibrium (Figure 12b). Figure 12c shows how the binding isotherm depends on N in this regime when $\alpha = 1$, that is, there is no allosteric cooperativity. For high values of N and KEM, the system displays both molecular and macroscopic all-or-nothing behavior. In the limit of strong chelate cooperativity ($KEM \gg 1$), $\log c_R$ tends to $1 + 2/(N-1)$. In the limit of large values of N, a sharp nucleation point is observed and $\log c_R = 1$ (Figure 12c green line). Although the distribution of K values for the formation of discrete closed oligomers is different from that for polydisperse open aggregates, the macroscopic cooperativity exhibited by the open and closed systems is practically identical. For example, the binding isotherm for $N = 8$ in Figure 12c (black line) is the same as that for $\alpha = 100$ in Figure 8b (blue line). Thus for $N > 2$, chelate cooperativity in the self-assembly of a closed cyclic complex is indistinguishable, at the macroscopic level, from positive allosteric cooperativity in the formation of polydisperse open oligomers.

The behavior of these systems is not affected by increasing the number of interaction sites per molecule, and this model describes a wide variety of self-assembled architectures. Chelate cooperativity has been investigated in supramolecular systems such as helicates[7,29] and ladders.[30] Fujita's cages illustrate the type of process described in Figure 12b.[31]

2.5. Denaturation

Finally, we consider processes in which a monovalent ligand breaks up a supramolecular assembly (as in the unfolding of a protein by addition of guanidine hydrochloride, Figure 2b). Again we start by considering the simplest possible system: the competition between a monovalent ligand (B) and a divalent ligand (BB) for a two-site receptor (AA), Figure 13. This competition allows us to make a direct

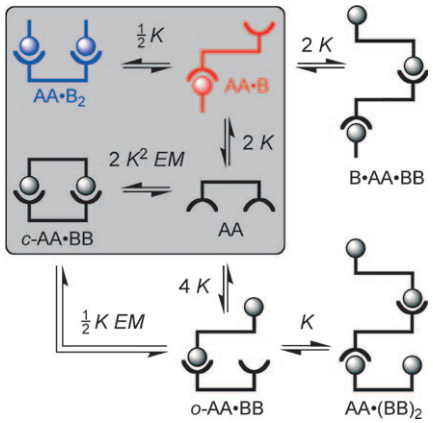

Figure 13. Competition between ligands with one and two binding sites (B and BB respectively) for a two-site receptor (AA).[12] Many species are possible, but if $[BB]_0 \gg [AA]_0$ and $KEM \gg 1$, then the only states of the receptor that are significantly populated are AA, *c*-AA·BB, AA·B, and $AA{\cdot}B_2$.

comparison between the two types of cooperativity discussed in Sections 2.2–2.4. In the denaturation experiment, B is added to the AA·BB complex to displace BB from the receptor. A large number of different states are possible, but we will consider the scenario where the ligand is present in a large excess relative to the receptor, such that $[BB]_0 \gg [AA]_0$. Under these conditions, only four states are populated to any significant extent (highlighted in the box in Figure 13).

The behavior of the system depends on the values of the molecular parameters α and KEM, but we restrict ourselves to the case of $\alpha = 1$, where binding of B to AA is non-cooperative in the absence of BB. Two limiting regimes are illustrated in Figure 14.

KEM $\ll 1$ (Figure 14a). Under these conditions, BB is not strongly bound to AA, so formation of $AA{\cdot}B_2$ is unaffected by the presence of BB. The speciation profile is identical to the non-cooperative system (compare Figure 4b and Figure 14a). It is possible to construct a Hill plot for the interaction of B with the AA·BB complex. Complexation is not cooperative ($n_H = 1$ and $\log c_R = 2$).

KEM $\gg 1$ (Figure 14b). Now only two states of the receptor are present at significant concentrations: the cyclic complex *c*-AA·BB and the 1:2 complex $AA{\cdot}B_2$. Binding of the first molecule of B competes with the cooperative intramolecular interaction between AA and BB in the doubly linked *c*-AA·BB complex, whereas binding of the second molecule of B competes with the non-cooperative intermolecular interaction between AA and BB in the singly linked B·AA·BB. The speciation profile for this system is identical to the profile obtained for an allosteric system with positive cooperativity (compare Figure 4d and Figure 14b). Under these conditions, the denaturation system shows all the

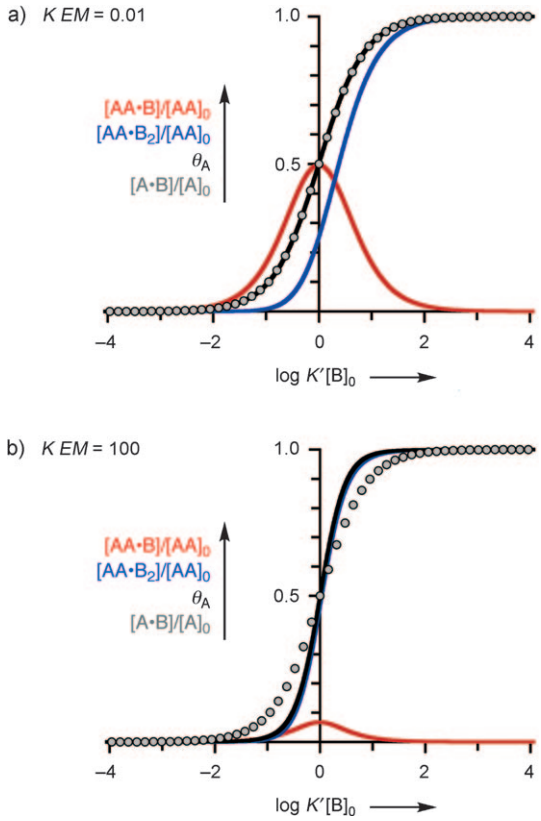

Figure 14. Speciation profiles for the denaturation of AA·BB by addition of B (equilibria in Figure 13; AA·B in red, AA·B_2 in blue, and total binding site occupancy θ_A for sites of AA occupied by B in black). The speciation profile for the system with one intermolecular interaction is shown for reference (gray dots). a) $KEM = 0.01$; b) $KEM = 100$ (in this case, the black and the blue curves are practically identical). $\alpha = 1$; $K = 1\ M^{-1}$, $[BB]_0 = 1$ M, and $[AA]_0 = 0.1$ M.[14]

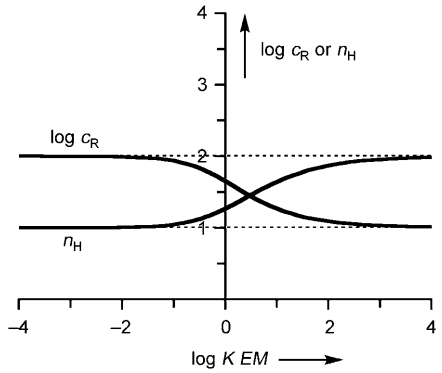

Figure 15. Relationship between the molecular parameter KEM and the macroscopic parameters n_H and c_R for the denaturation of the self-assembled complex *c*-AA·BB by a monovalent ligand B.

macroscopic hallmarks of positive cooperativity ($n_H > 1$ and $\log c_R < 2$). It is important to note that $\alpha = 1$ in this example, and so the macroscopic cooperativity observed for the binding of B is solely a consequence of the chelate cooperativity associated with self-assembly of the *c*-AA·BB complex.

The relationships between the macroscopic indicators of cooperativity n_H and c_R (for the binding of B to the *c*-AA·BB complex) and KEM (the molecular parameter that quantifies the chelate cooperativity in the binding of BB to AA) are shown in Figure 15. When $KEM \ll 1$, simple non-cooperative binding of B is observed; $n_H = 1$ and $\log c_R = 2$. The Hill coefficient n_H increases with KEM and tends to a limiting value of 2; $\log c_R$ decreases as KEM increases and tends to a lower limit of 1. In the strong chelate cooperativity regime, the relationships of n_H and c_R with KEM shown in Figure 15 are strikingly similar to the relationships of n_H and c_R with α shown in Figure 6. KEM and α are analogous measures of two different types of cooperativity, and the denaturation experiment reveals how they are related. Comparison of Figure 6 and Figure 15 shows that allosteric cooperativity can be positive or negative (depending on whether $\alpha > 1$), whereas chelate cooperativity is positive for all values of KEM.

The behavior of this system can be generalized to any number (N) of interaction sites. For example, consider denaturation of the 1:1 complex of a polytopic receptor (A···A) and a polyvalent ligand B···B (Figure 16a). If $KEM \ll 1$, cooperative self-assembly does not take place, and denaturant binding is non-cooperative ($n_H = 1$ and $\log c_R = 2$). However if $KEM \gg 1$, denaturant binding competes with cooperative self-assembly, and the denaturation isotherm shows all the macroscopic hallmarks of positive allosteric cooperativity. Binding isotherms for different values of N are shown in Figure 16b. In the limit of strong chelate cooperativity, n_H tends to a value of N, and $\log c_R$ tends to a value of $2/N$. Binding of the Nth denaturant competes with an intermolecular interaction, whereas binding of the first ($N-1$)

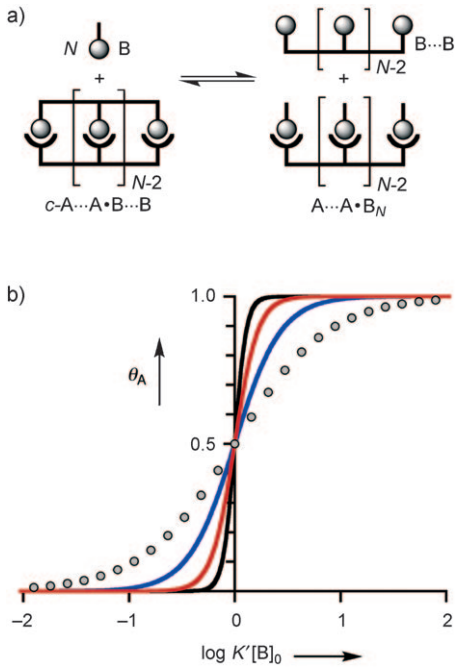

Figure 16. a) Denaturation of a 1:1 complex of a polytopic receptor A···A and a complementary polyvalent ligand B···B, both with N binding sites in the limit of strong chelate cooperativity. b) Denaturant site occupancy θ_A profiles plotted for $N = 1$ (gray dots), $N = 2$ (blue), $N = 4$ (red), and $N = 8$ (black).[14]

denaturants compete with intramolecular interactions. Thus, the positive macroscopic cooperativity is a consequence of the strong binding interaction with the final ligand.

Similar behavior is observed for the denaturation of any self-assembled structure held together by cooperative intramolecular interactions, regardless of the architecture.

Denaturation is widely used to measure the stability of biopolymer assemblies, such as proteins[32] and oligonucleotides.[33] Often these are two-state equilibria, and Hill coefficients can be used to quantify their cooperativity. For example, the data for denaturation of lysozyme by guanidine hydrochloride plotted in Figure 2b[11] gives a linear Hill plot in the range $0.1 < \theta_A < 0.9$ with $n_H = 17$. This result implies that each lysozyme molecule binds at least 17 molecules of guanidine hydrochloride on denaturation. However, there are problems with the interpretation of protein denaturation in terms of binding models, because the protein does not have discrete binding sites for the denaturant, and the activity of the denaturant may not be proportional to its concentration.[34] In practice, the cooperativity of protein denaturation is generally analyzed in terms of the empirical relationship in Equation (9):[32,35]

$$-RT\ln\{\theta_A/(1-\theta_A)\} = \Delta G - m[B]_0 \quad (9)$$

where $-RT\ln\{\theta_A/(1-\theta_A)\}$ is the free energy of protein folding at a concentration of denaturant of $[B]_0$, ΔG is the free energy of folding in the absence of the denaturant, and m is a macroscopic cooperativity parameter, which is found to be proportional to the change in the solvent-accessible surface area on unfolding.[35]

Surprisingly few denaturation experiments have been reported for supramolecular systems. Whitesides and coworkers have studied cooperativity in self-assembled H-bonded complexes using DMSO denaturation.[36] The cooperative formation of supramolecular ladders has been probed by denaturation,[30] and binding curves for the displacement of multivalent ligands from cyclic porphyrin oligomers with pyridine match the simulated curves in Figure 16.[37]

3. Standard State Considerations

The relationship between allosteric and chelate cooperativity is illustrated by considering free energies. Here we compare the free energy of formation of the complexes $AA{\cdot}B_2$ and c-AA·BB (Figure 4a and Figure 9). The free energy of formation of $AA{\cdot}B_2$ is given by Equations (10) and (11):

$$\Delta G_{AA{\cdot}B_2} = -RT\ln(\alpha K^2) \quad (10)$$

$$= 2\Delta G_{A{\cdot}B} - RT\ln(\alpha) \quad (11)$$

Positive cooperativity ($\alpha > 1$) arises when the free energy of formation of the assembly is more than the sum of the free energies of the isolated interactions. Equations (12)–(14) describe the corresponding case for formation of c-AA·BB with $\alpha = 1$:

$$\Delta G_{c\text{-}AA{\cdot}BB} = -RT\ln(2EM\ K^2) \quad (12)$$

$$= 2\Delta G_{A{\cdot}B} - RT\ln(2EM) \quad (13)$$

$$= \Delta G_{A{\cdot}B} - RT\ln(2K\ EM) \quad (14)$$

The apparent similarity of Equations (11) and (13) is deceptive. Whereas α is the dimensionless ratio of two bimolecular association constants, EM has units of concentration, so the sign of $\ln(2EM)$ depends on the choice of standard state. The situation where $2EM = 1$ M has no special significance. The dimensionless parameter that characterizes cooperativity in self-assembled systems is the product KEM, so Equation (13) should be rewritten as Equation (14). The significance of the situation where $(2KEM) = 1$ is that it is the threshold below which self-assembly does not perturb the properties of the system. The thermodynamic analysis of complexes with different numbers of components and interactions is a common source of confusion: *cooperativity in self-assembled systems should be quantified by the dimensionless product KEM rather than EM.*

4. Conclusions

In this Essay, we have examined the two distinct types of cooperativity that determine the speciation in supramolecular and biological systems: *allosteric* and *chelate* cooperativity. Chelate cooperativity is a feature of closed self-assembled structures and operates even when the microscopic affinities of the binding sites for monovalent ligands are all identical. We have shown that chelate cooperativity can lead to macroscopic behavior that is indistinguishable from that of positive allosteric cooperativity. This is evident from the concentration dependence of the self-assembly of closed oligomers c-$(AB)_N$ (Figure 12) and from the denaturation of self-assembled complexes c-AA·BB by addition of a denaturant (Figure 14 and Figure 16). If one were only able to observe the overall fraction of bound receptor sites θ_A as a function of the ligand concentration, then one would not be able to distinguish chelate cooperativity from allosteric cooperativity (compare Figure 8b with Figure 12c, Figure 4d with Figure 14b, and Figure 7 with Figure 16b). In the limit of strong positive cooperativity, a characteristic two-state speciation profile with a stoichiometry-determined shape is observed for allosteric ligand binding to a polytopic receptor, self-assembly of an oligomeric complex, and denaturation of a structure held together by multiple intermolecular interactions.

Experimentally, both types of cooperativity can be observed from the Hill coefficient n_H and the concentration switching window c_R. At the molecular level, allosteric cooperativity is characterized by the interaction parameter α, while chelate cooperativity is characterized by product KEM. In allosteric systems, cooperativity can be either positive or negative, depending on the value of α, whereas chelate cooperativity can only be positive. Comparison of allosteric binding with denaturation of self-assembled complexes reveals that the relationships of the macroscopic

parameters n_H and c_R with α are very similar to the relationships with KEM. In the limit of strong positive cooperativity ($\alpha \gg 1$ or $KEM \gg 1$), the stoichiometry of the complex (N) can be determined from titration experiments, where n_H tends to $(N-1)$ and $\log c_R$ tends to $2/(N-1)$, or from dilution experiments, where $\log c_R$ tends to $1+2/(N-1)$.

There are two cases in which the macroscopic parameters n_H and c_R do not provide insight into the cooperativity that is present at the molecular level: unimolecular folding and bimolecular self-assembly. The former is independent of concentration, and because the stoichiometry of the latter is two, the binding isotherms have the same form as non-cooperative binding that involves only one intermolecular interaction. However, the presence of chelate cooperativity in both cases can be revealed by denaturation.

The link between allosteric and chelate cooperativity is exemplified by hemoglobin.[1] Chelate cooperativity in hemoglobin leads to formation of a self-assembled tetrameric protein (Figure 1c). In mammalian hemoglobin, each part of the tetramer binds oxygen in an allosteric manner (Figures 1a and 2a). In hemoglobin from lamprey fish, oxygen binding causes the four subunits to dissociate, and cooperativity in ligand binding is associated with denaturation of the tetramer (Figure 17). In this case, the frame of reference determines whether the cooperativity is described as positive or negative: as far as the ligand is concerned, the binding of one oxygen molecule increases the affinity of the receptor for other oxygen molecules (*positive homotopic cooperativity*); as far as the receptor is concerned, the binding of one oxygen molecule reduces the affinity of one hemoglobin monomer for another hemoglobin monomer (*negative heterotopic cooperativity*).[6] Tabushi exploited the link between allosteric and chelate cooperativity by showing that hemoglobin-like cooperativity can be achieved using oxygen as a monovalent ligand to displace a chelated divalent ligand from a metalloporphyrin dimer (see Figure 13).[38]

Allosteric cooperativity is widely recognized, and its definition is unambiguous.[5] However, there has been a tendency to define cooperativity in such a way as to exclude chelate effects. At the molecular level, chelate and allosteric effects are completely different, but they can result in identical macroscopic cooperative behavior. Furthermore, most natural and artificial examples of strong positive cooperativity are cases of chelate cooperativity. Typical microscopic association constants in supramolecular systems are in the range 10^2–$10^4\,M^{-1}$ with typical effective molarities in the range 10^{-3}–$10^1\,M$,[39] which lead to KEM values of 10^{-1}–10^5, whereas the value of α is typically 10^{-3}–10^2.[10,21] Many apparent cases of strong positive allosteric cooperativity actually involve chelation. For example, highly cooperative nucleation–growth of open linear aggregates usually involves the formation of helical or multistrand oligomers with closed loops of intramolecular chelate interactions.[22,23,40]

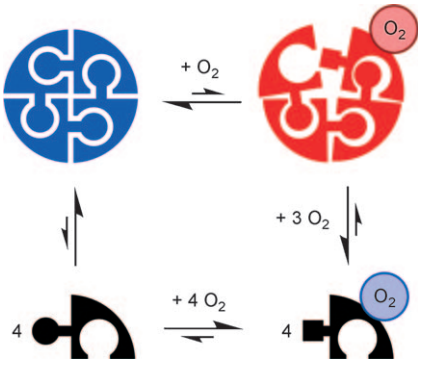

Figure 17. Lamprey hemoglobin forms a self-assembled tetramer (top), but oxygen binding (right) competes with subunit interactions. The monomer has a higher affinity for oxygen than the tetramer, so the species that dominate are the free tetramer and bound monomer. The chelate cooperativity that stabilizes the tetramer leads to positive allosteric cooperativity in oxygen binding.

In reality, chelate and allosteric effects often exist together in the same system. When the cooperating interaction sites are far apart, cooperativity is easy to quantify, as discussed above. However, when the sites are close together, this analysis becomes difficult, because an appropriate single-site reference system may not be available. Consider a guanine–cytosine base-pair for example. There is allosteric cooperativity, which arises from secondary electrostatic interactions between neighboring H-bond sites,[41] and chelate cooperativity, which stabilizes the triply H-bonded state relative to partially bound intermediates. However, dissection of the contributions of KEM and α is problematic because of the difficulty in selecting the reference systems required to estimate K values for the individual H-bond sites.[42]

The recognition of chelate cooperativity, as similar to, but different from, allosteric cooperativity, has important implications. For example, the realization that multivalent assemblies can be designed to exhibit sharp bound–free transitions is useful in the creation of responsive materials, sensors, or drug delivery systems, where small changes in conditions lead to an abrupt switch in binding. Cooperativity is also fundamental to understanding the operation of biological systems, where coordinated switching of molecular species between discrete states is the key to managing complexity.

Abbreviations

α	allosteric interaction parameter
[A]	concentration of species A (free)
$[A]_0$	total concentration of A, including free and A bound to other species.
c_R	concentration switching window
EM	effective molarity
K	association constant
K'	normalized association constant[14]
log	decadic logarithm
ln	natural logarithm
n_H	Hill coefficient
N	number of binding sites
R	gas constant
T	temperature
ΔG	free energy change of equilibrium
θ_A	site occupancy of receptor A

Received: May 11, 2009
Published online: September 10, 2009

[1] M. F. Perutz, *Q. Rev. Biophys.* **1989**, *22*, 139 – 236.
[2] S. Shinkai, M. Ikeda, A. Sugasaki, M. Takeuchi, *Acc. Chem. Res.* **2001**, *34*, 494 – 503.
[3] J. D. Badjic, A. Nelson, S. J. Cantrill, W. B. Turnbull, J. F. Stoddart, *Acc. Chem. Res.* **2005**, *38*, 723 – 732; A. Mulder, J. Huskens, D. N. Reinhoudt, *Org. Biomol. Chem.* **2004**, *2*, 3409 – 3424.
[4] M. Mammen, S.-K. Choi, G. M. Whitesides, *Angew. Chem.* **1998**, *110*, 2908 – 2953; *Angew. Chem. Int. Ed.* **1998**, *37*, 2754 – 2794.
[5] G. Ercolani, *J. Am. Chem. Soc.* **2003**, *125*, 16097 – 16103.
[6] D. H. Williams, E. Stephens, D. P. O'Brien, M. Zhou, *Angew. Chem.* **2004**, *116*, 6760 – 6782; *Angew. Chem. Int. Ed.* **2004**, *43*, 6596 – 6616.
[7] J. Hamacek, M. Borkovec, C. Piguet, *Dalton Trans.* **2006**, 1473 – 1490.
[8] A. Whitty, *Nat. Chem. Biol.* **2008**, *4*, 435 – 439.
[9] J. M. Berg, J. L. Tymoczko, L. Stryer, Biochemistry, 6th ed., Freeman, New York, **2007**.
[10] F. J. W. Roughton, R. L. J. Lyster, *Hvalradets Skr.* **1965**, *48*, 185 – 198.
[11] M. Ikeguchi, K. Kumajima, S. Sugai, *J. Biochem.* **1986**, *99*, 1191 – 1201.
[12] Statistical factors for equilibria such as those in Figures 4a, 7, 9, 11, 12, 13, and 16a are readily calculated from symmetry numbers, as explained in the Supporting Information; see: S. W. Benson, *J. Am. Chem. Soc.* **1958**, *80*, 5151 – 5154; W. F. Bailey, A. S. Monahan, *J. Chem. Educ.* **1978**, *55*, 489 – 493; G. Ercolani, C. Piguet, M. Borkovec, J. Hamacek, *J. Phys. Chem. B* **2007**, *111*, 12195 – 12203.
[13] K. A. Connors, A. Paulson, D. Toledo-Velasquez, *J. Org. Chem.* **1988**, *53*, 2023 – 2026.
[14] The concentration scales in the plots are normalized by the apparent association constant per site K', where $1/K'$ is the concentration at $\theta_A = 50\,\%$.
[15] A. V. Hill, *Biochem. J.* **1913**, *7*, 471 – 480; L. D. Byers, *J. Chem. Educ.* **1977**, *54*, 352 – 354.
[16] We define c_R using the change from 1:10 to 10:1 in the bound/free ratio rather than the 1:9 to 9:1 originally suggested by K. Taketa, B. M. Pogell, *J. Biol. Chem.* **1965**, *240*, 651 – 662.
[17] The decrease in c_R with increasing N for complexes of the type $A\cdots A{\cdot}B_N$ is analogous to the decrease in the potential gap between the oxidation and reduction waves in cyclic voltammetry, with increasing number of electrons (N), according to the equation $\Delta E = 57/N$ mV.
[18] D. H. Williams, A. J. Maguire, W. Tsuzuki, M. S. Westwell, *Science* **1998**, *280*, 711 – 714.
[19] J. Rebek, T. Costello, L. Marshall, R. Wattley, R. C. Gadwood, K. Onan, *J. Am. Chem. Soc.* **1985**, *107*, 7481 – 7487.
[20] A. P. Bisson, C. A. Hunter, J. C. Morales, K. Young, *Chem. Eur. J.* **1998**, *4*, 845 – 851.
[21] E. Terzi, G. Hölzemann, J. Seelig, *J. Mol. Biol.* **1995**, *252*, 633 – 642.
[22] D. Zhao, J. S. Moore, *Org. Biomol. Chem.* **2003**, *1*, 3471 – 3491.
[23] P. Jonkheijm, P. van der Schoot, A. P. H. J. Schenning, E. W. Meijer, *Science* **2006**, *313*, 80 – 83; M. M. J. Smulders, A. P. H. J. Schenning, E. W. Meijer, *J. Am. Chem. Soc.* **2008**, *130*, 606 – 611.
[24] Z. Chen, A. Lohr, C. R. Saha-Möller, F. Würthner, *Chem. Soc. Rev.* **2009**, *38*, 564 – 584.
[25] V. Simic, L. Bouteiller, M. Jalabert, *J. Am. Chem. Soc.* **2003**, *125*, 13148 – 13154; M. de Loos, J. van Esch, R. M. Kellogg, B. L. Feringa, *Angew. Chem.* **2001**, *113*, 633 – 636; *Angew. Chem. Int. Ed.* **2001**, *40*, 613 – 616.
[26] The effective molarity EM is usually estimated using Equations (15) or (16):

$$EM = K_o\, K(c\text{-}AA{\cdot}BB)/K(AA{\cdot}B_2) \qquad (15);$$
$$EM = K_o\, K(c\text{-}AA{\cdot}BB)/K(A{\cdot}B)^2 \qquad (16).$$

For complexes where the binding sites are identical, there is a statistical factor ($K_o = 2$), which accounts for the difference in binding site concentration between a monovalent ligand (B) and a divalent ligand (BB).[12] Some authors incorporate the statistical factor into the value of EM.
[27] In Figure 10, θ_A is defined by the equation:

$$\theta_A = \frac{1/2\,[o\text{-}AA{\cdot}BB] + [c\text{-}AA{\cdot}BB] + [AA{\cdot}(BB)_2]}{[AA]_0} \qquad (17).$$

[28] B. Zhang, R. Breslow, *J. Am. Chem. Soc.* **1993**, *115*, 9353 – 9354.
[29] A. Pfeil, J.-M. Lehn, *J. Chem. Soc. Chem. Commun.* **1992**, 838 – 840; N. Fatin-Rouge, S. Blanc, A. Pfeil, A. Rigault, A.-M. Albrecht-Gary, J.-M. Lehn, *Helv. Chim. Acta* **2001**, *84*, 1694 – 1711.
[30] P. N. Taylor, H. L. Anderson, *J. Am. Chem. Soc.* **1999**, *121*, 11538 – 11545; T. E. O. Screen, J. R. G. Thorne, R. G. Denning, D. G. Bucknall, H. L. Anderson, *J. Mater. Chem.* **2003**, *13*, 2796 – 2808; A. Camara-Campos, C. A. Hunter, S. Tomas, *Proc. Natl. Acad. Sci. USA* **2006**, *103*, 3034 – 3038.
[31] M. Fujita, M. Tominaga, A. Hori, B. Therrien, *Acc. Chem. Res.* **2005**, *38*, 369 – 378.
[32] D. Barrick, *Phys. Biol.* **2009**, *6*, 015001.
[33] V. M. Shelton, T. R. Sosnick, T. Pan, *Biochemistry* **1999**, *38*, 16831 – 16839.
[34] J. A. Schellman, *Biopolymers* **1978**, *17*, 1305 – 1322.
[35] J. K. Myers, C. N. Pace, J. M. Scholtz, *Protein Sci.* **1995**, *4*, 2138 – 2148.
[36] M. Mammen, E. E. Simanek, G. M. Whitesides, *J. Am. Chem. Soc.* **1996**, *118*, 12614 – 12623.
[37] M. Hoffmann, J. Kärnbratt, M.-H. Chang, L. M. Herz, B. Albinsson, H. L. Anderson, *Angew. Chem.* **2008**, *120*, 5071 – 5074; *Angew. Chem. Int. Ed.* **2008**, *47*, 4993 – 4996; M. Hoffmann, C. J. Wilson, B. Odell, H. L. Anderson, *Angew. Chem.* **2007**, *119*, 3183 – 3186; *Angew. Chem. Int. Ed.* **2007**, *46*, 3122 – 3125.
[38] I. Tabushi, T. Sasaki, *J. Am. Chem. Soc.* **1983**, *105*, 2901 – 2902; I. Tabushi, *Pure Appl. Chem.* **1988**, *60*, 581 – 586.
[39] K. N. Houk, A. G. Leach, S. P. Kim, X. Zhang, *Angew. Chem.* **2003**, *115*, 5020 – 5046; *Angew. Chem. Int. Ed.* **2003**, *42*, 4872 – 4897.
[40] T. E. Kaiser, V. Stepanenko, F. Würthner, *J. Am. Chem. Soc.* **2009**, *131*, 6719 – 6734.
[41] W. L. Jorgensen, J. Pranata, *J. Am. Chem. Soc.* **1990**, *112*, 2008 – 2010.
[42] J. R. Quinn, S. C. Zimmerman, J. E. Del Bene, I. Shavitt, *J. Am. Chem. Soc.* **2007**, *129*, 934 – 941.